Benchmarking of hydrogen selective membranes: Experimental and modelling approach to compare membrane performance

J. Boon **(ECN)**
J.A.Z. Pieterse **(ECN)**
J.W. Dijkstra **(ECN)**
Y.C. van Delft **(ECN)**
P. Veenstra **(Shell)**
A. Nijmeijer **(Shell)**
D. Jansen **(ECN)**

August 2013
ECN-W--13-040

Available online at www.sciencedirect.com

SciVerse ScienceDirect

Energy Procedia 37 (2013) 1020 – 1029

Energy Procedia

GHGT-11

Benchmarking of hydrogen selective membranes: Experimental and modelling approach to compare membrane performance

J. Boon[a], J.A.Z. Pieterse[a*], J.W. Dijkstra[a], Y.C. Van Delft[a], P. Veenstra[b], A. Nijmeijer[b], D. Jansen[a]

[a] *ECN, P.O. Box 1, NL 1755 ZG Petten, The Netherlands*

[b] *Shell Global Solutions International B.V., P.O. Box 3800, 1030 BN Amsterdam, The Netherlands*

Abstract

Precombustion CO_2 capture can be feasible with mature palladium-based membranes in modules. Before moving on to demonstration, benchmarking of membranes is a crucial step in their introduction. The strategy presented here, consisting of matching results from experiments and model development, will be a valuable tool in benchmarking membrane performance. Using experiments with pure hydrogen feed and no sweep, the permeation of hydrogen through the metallic palladium layer was accurately fitted with a standard permeation equation (1) with Q and n as regressed parameters. The pressure drop in the membrane support was included but was found to be small (14 kPa). Hydrogen-nitrogen separation experiments without sweep gas could be predicted by a 2D laminar flow convection and diffusion model. Thus, convective and diffusive transport of hydrogen and inert in the modules was successfully accounted for by the module model. Experiments with nitrogen sweep gas have shown significant resistances in the membrane support. These were predicted by the dusty gas model to be both a small pressure drop and a rather large mole fraction gradient in the support layer, the latter being far more important than the former. The derived model allows to quantify, as a function of operating conditions, the intrinsic and external mass transfer resistances. In order to make the final step toward full use of the model in benchmarking of membranes the model is currently be extended to incorporate the effect of inhibition of syngas components. The final model will be used to run selected cases and the results will be validated with hydrogen permeation results from experiments in syngas. The model will also be used for predicting membrane performance at commercial scale.

Keywords: Hydrogen; precombustion decarbonization; palladium membranes; modelling; benchmark

*Corresponding author. Tel.:+31-224-568154

E-mail address: pieterse@ecn.nl

Selection and/or peer-review under responsibility of GHGT
doi:10.1016/j.egypro.2013.05.198

1. Introduction

Palladium alloy membranes are a promising option for hydrogen separation in industrial hydrogen production and in pre-combustion CO_2 capture [1,2]. Given the state of the art, benchmarking of membranes from different vendors is a crucial step in the introduction of hydrogen membranes to demonstrate the maturity and performance under industrially relevant conditions. A multitude of membrane manufacturers and developers exists, yet at the moment, performance figures have been published at different conditions, and including the impact of externals, e.g. different membrane module designs. Resistances to mass transfer will become increasingly important with the increasing flux and modeling provides the fundamental understanding of the prevailing mass transfer processes to design and operate membrane units [3,4]. The present contribution provides an overview of the benchmark approach to assess the performance of H_2-selective membranes under industrially relevant conditions, independent from the impact of module design.

Membranes were tested at a scale of a few hundred square centimeters in the process development unit (PDU) setup at ECN [5] capable of accommodating up to 8 membranes of 50 cm length in parallel, see Figure 1. Process conditions were varied systematically. Starting with pure H_2 feed and without sweep, N_2 was sequentially introduced as inert on the feed side and as sweep gas, respectively. Finally, H_2 separation from syngas mixtures was measured, containing gas phase constituents as present in pre-combustion syngas streams.

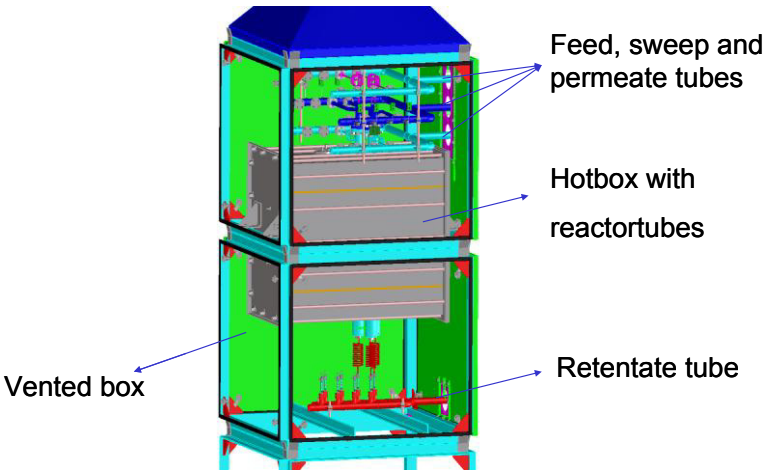

Fig. 1 Multitube membrane test setup

For pure H_2, the observed flux is converted into a permeance for the Pd layer, using a phenomenological description. In presence of other species, the observed flux may be lowered by mass transfer resistances or surface inhibition. Gas phase mass transfer in the module is dependent on module design, scale and other operation conditions. To obtain performance data of the membrane itself, this should be taken out of consideration. On the other hand, mass transfer resistance in the support and inhibition are an inherent property of the membrane and should therefore be included in the membrane performance assessment. The staged experimental approach, schematically depicted in Figure 2, allows for investigating systematically the effects of intrinsic permeation, hydrodynamics, and concentration polarization. It thus supports model development and leads to improved understanding of the important phenomena that direct the permeation of H_2. This approach will allow benchmarking of membranes by

translating the complex flux equations to the membrane area required to reach target recoveries for selected useful cases.

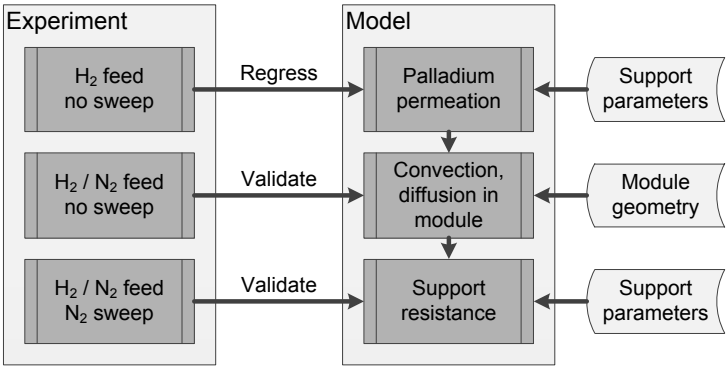

Fig. 2 Research strategy, systematically the effects of intrinsic permeation, hydrodynamics, and concentration polarization

2. Experimental

2.1 Membranes and modules

Membranes were obtained from membrane developers. They mostly consist of a thin (several micron) layer of palladium(-alloy) on a ceramic or porous stainless steel support tube. In the present contribution the results presented are limited to results obtained with ECN (Hysep) membranes [6], serving as example of typical test results. They consist of a thin (3–9 micron) layer of palladium on a ceramic support tube [7].The support tubes are ceramic tubes of 14 mm outer diameter and 2 mm thickness and contain three layers of different structure. The properties of the support tube layers have been summarized in [6]. Three membranes have been used in a parallel configuration. After sealing [8], the effective length of each of the membranes is approximately 45 cm, giving a total surface area for three membranes of 595 cm^2. Each of the membrane tubes was mounted in a cylindrically shaped module (see Figure 3). An insert tube is used for the sweep gas, creating a double annulus geometry enclosing the membrane. The use of multiple membranes serves to achieve suitable total membrane surface areas for the workable flow ranges of the test rig. In these conditions, the Reynolds number varies up to a maximum of 1100, assuring laminar flow conditions in all experiments.

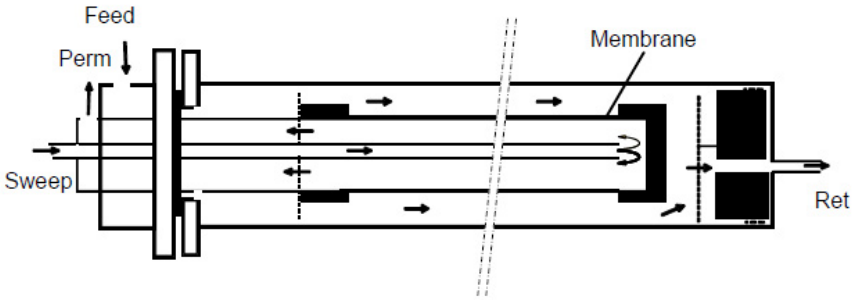

Fig. 3. Cross-section of the PDU membrane module

2.2 Test procedure

Experiments have been performed on ECN's 'Process Development Unit' (PDU), described in more detail elsewhere [9, 10]. The modules were placed in an electrically heated oven at 400 °C, with a maximum temperature gradient over the module length of 25°C. H_2 and N_2 were fed by Bronkhorst (the Netherlands) mass flow controllers. Gas distribution over the three modules was controlled by orifices and uniform. The pressures on the retentate and permeate side were controlled by a back pressure control (Bronkhorst) and measured at the module outlets with a pressure transducer (Swagelok, USA). Data with a deviation between pressure control and measurement of more than 10% of the pressure difference over the membrane were discarded.
The gas flow rate in the retentate and permeate has been measured by mass flow meters (Bronkhorst). The gas composition of the total retentate and permeate flows as well as that of the stream exiting the individual membrane tubes was determined with a gas chromatograph (HP, P200H) equipped with a molsieve column, a Poraplot column and a TCD detector. In addition, an Advance Optima online analysis (ABB Magnos106) was used to monitor the concentration of H_2 with a Caldos 4T-EX detector. Process values have been recorded when for five minutes the pressures were stable (±5 kPa) and the measured flows were stable (±0.03 Nl min^{-1}), and the measurements have been repeated three times. H_2 and N_2 mass balance assessments with representative gas mixtures during test runs have shown to be mostly within 5%. Incidental measurements with a mass balance error more than ± 7% have been discarded. After a leak test at room temperature the membranes have been purged with N_2 on the feed and permeate side to remove air from the system. Subsequently, the reactor was heated to 400°C with a ramp of 1°C min^{-1} while applying a N_2 flow at the feed and sweep side, followed by a pure N_2 leak test. With a retentate pressure of 0.6 MPa and a permeate pressure of 0.11 MPa, a leak rate of 0.02 Nl min^{-1} was found. After the separation tests, the N_2 leak test was repeated at 0.6 MPa and 0.15 MPa, yielding a leak rate of 0.20 Nl min^{-1}. Although there is a small increase in the leak rate, a high selectivity is maintained throughout the experiments and a correction of the experimental results for leak flow was therefore not necessary. After the first leak test at 400°C, the feed and permeate side were purged with 20 Nl min^{-1} of H_2 for 30 minutes in order to remove the remaining N_2, followed by a stabilization period of 23 hours in 0.21/0.11 MPa of H_2 (20 Nl min^{-1} of H_2 on the feed side, no sweep) and measurement of the pure H_2 permeance of the membranes every two hours. After stabilization, pure H_2 permeance tests were done at 400°C. Then gas mixtures of 55% H_2 in N_2 were tested, varying retentate and permeate pressures, feed flow and sweep flow rates. To make sure no trends would be induced by the measurement history, the order of the experiments was randomized. Subsequently, syngas gas mixtures were tested, varying retentate and permeate pressures, feed flow and sweep flow rates.

2.3 Modelling

A model has been developed for the interpretation of the role of the different mass transfer resistances in the experiments. Inside the membrane itself, the palladium layer and the support layers are mass transfer resistances in series. Laminar convection and diffusion, i.e. concentration polarization, in the module are accounted for by solving the mass and momentum balances, assuming 2D axial symmetry.

2.3.1 Palladium layer

The mechanisms by which H_2 crosses the metallic palladium separation layer are complex and their modelling is inherently challenging. A number of sequential steps may be discerned according to Ward and Dao [11]:

- dissociative adsorption of H_2 on the Pd surface at the retentate side,
- transition of H atoms from the surface into the Pd bulk,
- diffusion through the Pd bulk,
- transition of H atoms from the bulk to the Pd surface at the permeate side, and
- recombinative desorption from the metal surface.

The individual steps have very different kinetics, and the overall kinetics depend on their relative importance. Ward and Dao [11] have made a detailed model for each of the steps and concluded that the diffusion of H atoms through the Pd bulk is rate-limiting, at least for a clean Pd layer with a thickness down to 1 micron and temperatures above 300 °C. In such a case, overall kinetics will obey Sieverts' law(1),

$$N_m = Q\left(p_{H_2,r}^{n} - p_{H_2,p}^{n}\right) \tag{1}$$

with n = 0.5 [12]. Here, N_m is the transmembrane flux, defined at the radial coordinate of the palladium layer, Q(T) is the temperature-dependent permeance, P_{H2},r and P_{H2},p are the retentate-side and permeate-side H_2 partial pressures, respectively. Later authors have added that, at higher H_2 partial pressures, corrections for the nonideality of the H-Pd system, surface effects, or thermal effects will lead to increased values of n [13,14,15,16]. For the purpose of the present study, it is sufficient to fit the parameters Q and n in the equation to experimental pure H_2 permeation data.

After H_2 molecules desorb from the metallic palladium separation layer on the permeate side, they need to cross the porous ceramic support layer before they end up in the permeate stream. The driving forces for the transfer of H_2 across the support are gradients in mole fraction and pressure. These driving forces are balanced by the friction forces exerted by gas molecules and the porous medium, which can be described by the dusty gas model (DGM)(2), taking into account viscous flow, Knudsen diffusion, and molecular diffusion [17, 18].

$$\begin{cases} \dfrac{dp}{dr} = \dfrac{r_m N_m}{r D_{1M}^{e}}\left[-\dfrac{y_{H_2}}{RT}\left(1+\dfrac{B_0 p}{\mu D_{1M}^{e}}\right) - \dfrac{1-y_{H_2}}{RT}\left(1+\dfrac{B_0 p}{\mu D_{2M}^{e}}\right)\right]^{-1} \\ \dfrac{dy_{H_2}}{dr} = -\dfrac{y_{H_2}}{p}\left(1+\dfrac{B_0 p}{\mu D_{1M}^{e}}\right)\dfrac{dp}{dr} - \dfrac{r_m N_m RT}{rp}\left(\dfrac{1}{D_{1M}^{e}} + \dfrac{1-y_{H_2}}{D_{12}^{e}}\right) \end{cases} \tag{2}$$

Both the feed/retentate side and the countercurrent sweep/permeate side of the module have an annular shape. For description of fluid flow and mass transfer, 2D steady state isothermal differential mass and momentum balances are solved for both channels in cylindrical geometry.

$$\rho\left(\frac{1}{r}\frac{\partial}{\partial r}rv_r+\frac{\partial v_z}{\partial z}\right)=0 \qquad \text{continuity} \qquad (1)$$

$$\rho\left(v_r\frac{\partial v_z}{\partial r}+v_z\frac{\partial v_z}{\partial z}\right)=-\frac{\partial p}{\partial z}+\mu\left[\frac{1}{r}\frac{\partial}{\partial r}\left(r\frac{\partial v_z}{\partial r}\right)+\frac{\partial^2 v_z}{\partial z^2}\right] \qquad \text{motion} \qquad (2)$$

$$v_r\frac{\partial c_{H_2}}{\partial r}+v_z\frac{\partial c_{H_2}}{\partial z}=D_{H_2}\left(\frac{1}{r}\frac{\partial}{\partial r}\left(r\frac{\partial c_{H_2}}{\partial r}\right)+\frac{\partial^2 c_{H_2}}{\partial z^2}\right) \qquad \text{material balance} \qquad (3)$$

$$\frac{\partial}{\partial r}\left(\frac{\partial p}{\partial z}\right)=0 \qquad \text{no radial pressure gradient} \qquad (4)$$

3. Results and discussion

Pure H_2 experiments without sweep were done for determining the parameters in equation (1). Retentate and permeate pressures were varied in the range of 0.24–3.3 MPa, and 0.11–3.0 MPa, respectively. The pressure difference over the membrane was varied between 0.10 MPa and 0.38 MPa. H_2 fluxes were measured in the range of 0.22–0.85 mol m^{-2} s^{-1}. Using nonlinear regression, the permeation equation (1), and the support pressure drop equation (2), values for Q and n were determined. The equation fits the data points well as shown in Figure 4. The maximum pressure drop over the support layer as predicted with the DGM was 13.5 kPa. For these conditions, the predicted H_2 flux across the membrane in absence of a pressure drop over the support layer would be 3% higher than the current flux prediction. For ease of comparison with literature reports, the same procedure with n = 1was used to determine a linearized permeance of 2.5 10^{-6} mol m^{-2} s^{-1} Pa^{-1}.

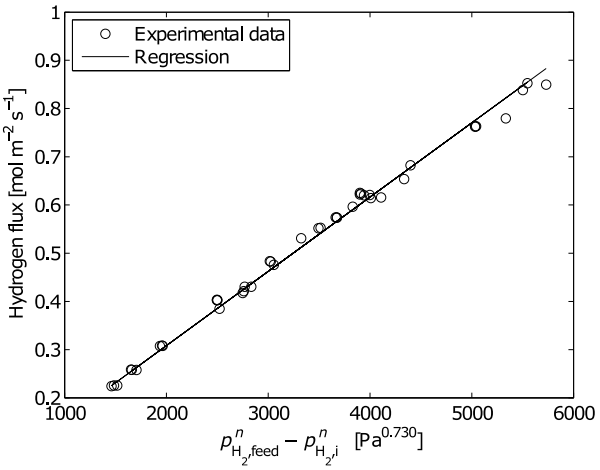

Fig. 4. Measured and regressed H_2 flux versus driving force; pure H_2, no sweep

The value of n = 0.730±0.007 is in line with values reported in literature for similar membranes and conditions [19,20]. The permeation equation (1) fits the data well. The model predicted pressure drop over the support layer in the pure H_2 experiments is relatively small, at a maximum of 13.5 kPa. The difference in flux caused by the pressure drop in the support amounts to only 3% and the pressure drop over the support layer could be ignored in assessing the pure H_2 measurements. Gas mixtures of 55% H_2 in N_2 were fed to the membranes at 3.0 MPa retentate pressure. The permeate side was controlled at 0.39–2.0 MPa, both without sweep gas and with 3–60 Nl min^{-1} of N_2 sweep. During all experiments, the feed flow was adjusted in the range of 20–80 Nl min^{-1} in order to have a H_2 recovery of 20–90%. The model was run in four modes. First, the model was run with gas phase convection and diffusion, but without accounting for mass transfer resistance in the support, which implies $dp/dr = 0$ and $dyH_2/dr = 0$ in equation (2) and leaving out the DGM altogether. The flux is then based directly upon the partial pressure difference between retentate and permeate sides. In the second and third mode, respectively, the resistances by pressure drop and diffusion were included. Finally, in the last mode, the full DGM was included for the membrane support, accounting for both the diffusional resistance and the pressure drop. Parity plots of the results for the first mode and the fourth mode versus measured fluxes are shown in Figure 5.

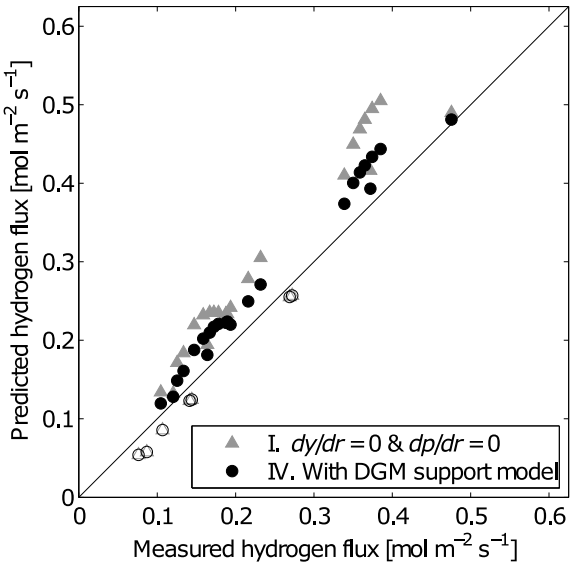

Fig. 5: Parity plot of predicted versus measured flux with H_2-N_2 feed, N_2 sweep; open symbols no sweep, closed symbols with N_2 sweep

A combination of the permeation model with the 2D module model in the first mode already gives good results for the cases without sweep gas. Clearly, both concentration polarization in the module and permeation through the membrane are accurately predicted. In contrast, the model predictions in the first mode do not represent the measurements with N_2 sweep. Including pressure drop over the membrane support in the second mode slightly improves the match (not shown), but a much greater improvement is made in the third mode (not shown), when the diffusional resistance by N_2 in the membrane support is included. Finally, the permeation model combined with the 2D module model and the support resistance

model based on the DGM (fourth mode) gives a prediction of the experimentally measured flux for all cases with an average error of 16.6%. Based on a comparison of the predicted fluxes with measured fluxes for the entire dataset, it can be concluded that the largest contribution of the support resistance for these experimental conditions results from the diffusional resistance due to penetration of sweep gas into the support. The effect of the resistance by the support matrix is negligible. The overall resistance to H_2 transfer from retentate to permeate is formed mainly by concentration polarization on the feed side, permeation across the palladium layer, and the diffusion barrier created by penetration of sweep gas in the membrane support. The feasible amount of sweep gas in any practical application must be determined based on the overall process, and by accounting for concentration polarization, permeation through the palladium, and membrane support resistance.

Hydrogen recovery values with the membranes have also been obtained with experiments carried out on the PDU with syngas mixtures and are shown in Figures 6 and 7. The feed gas composition used in the experiments was comparable to a composition for pre-combustion decarbonization in a power scheme for which natural gas is converted by autothermal reforming and subsequently pre-shifted downstream the membrane separator unit. Variation of feed flow (load to surface) (Figure 6) and permeate pressure (driving force of permeation) (Figure 7) were used to obtain insight in the conditional requirements to obtain H_2 recovery > 95 %. High hydrogen recovery is important to obtain a retentate stream enriched in CO_2. As can be noticed from Figure 6, the hydrogen recovery was 85 % at the highest achievable load to surface area in the PDU with the 595 cm^2 membrane area, using Ppermeate 19 bara and ΔP = 10 bar. The maximum recovery is easily increased towards 100 % by lowering the permeate pressure.

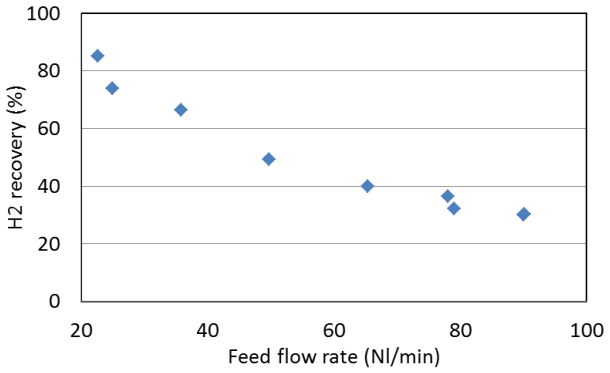

Fig.6: Hydrogen recovery versus feed flow rate. Syngas feed 4% CO; 19% CO_2; 18% H_2O; 55% H_2; 3%N_2 400 °C; L/S 38 Nml/min.cm^2; sweep 20 Nl/min N_2

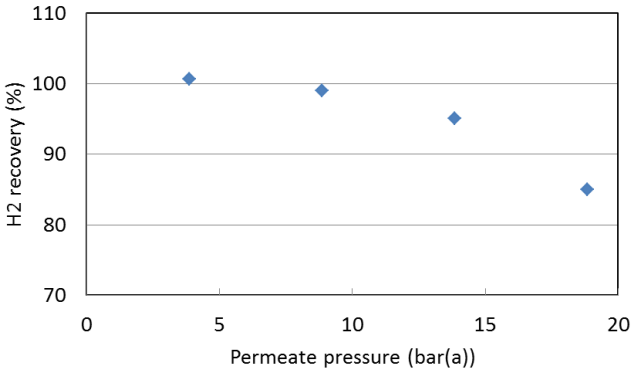

Fig.7: Hydrogen recovery versus permeate pressure. Syngas feed 4% CO; 19% CO_2; 18% H_2O; 55% H_2;3%N_2 400 °C; L/S 38 Nml/min.cm^2; sweep 20 Nl/min N_2

In order to 'benchmark' membranes provided by various vendors and developers, access the maturity of the technology and provide useful data for anticipated industrial pilot scale demonstration of the technology the experimental results obtained with membranes from various membrane developers need to be further interpreted by modeling. Each of these membranes have intrinsic permeance of H_2 through the Pd layer as well as mass transfer resistance through the support. Moreover, the various membranes of different membrane providers have different length, diameter and area and the modules used have different geometry. Therefore, each module performance is depending on mass transfer phenomena in the gas phase ('concentration polarisation') and load-to-surface ratio. The full 2D model will translate complex flux equations into required membrane area to reach target recovery for well-defined cases. The model for mass transfer in supported palladium-based membrane separators developed and validated in the present work already characterizes membranes and modules in great detail. In order to make the final step toward full use in benchmarking of membranes the model need to account for the effect of inhibition of syngas components, mainly CO. One or more syngas components may adsorb on the surface, thereby reducing the number of surface sites available for H_2 adsorption. It is generally reversible, and steady state is achieved within minutes. We are in the process of finalizing our model and running experiments with membrane (-modules) form various developers and the results of the benchmark will be available in the near future.

4. Conclusions

Using experiments with pure hydrogen feed and no sweep, the permeation of hydrogen through the metallic palladium layer was accurately fitted with a standard permeation equation (1) with Q and n as regressed parameters. The pressure drop in the membrane support was included but was found to be very small. Hydrogen-nitrogen separation experiments without sweep gas could be predicted by a 2D laminar flow convection and diffusion model. Thus, convective and diffusive transport of hydrogen and inert in the modules was successfully accounted for by the module model. Experiments with nitrogen sweep gas have shown significant resistances in the membrane support. These were predicted by the dusty gas model to be both a small pressure drop and a rather large mole fraction gradient in the support layer, the latter being far more important than the former. The derived model allows to quantify, as a function of operating conditions, the intrinsic and external mass transfer resistances. In order to make the final step toward full use of the model in benchmarking of membranes the model is currently be extended to

incorporate the effect of inhibition of syngas components. The final model will be used to run selected cases and the results will be validated with hydrogen permeation results from experiments in syngas. The model will also be used for predicting membrane performance at commercial scale.

Acknowledgements

Financial support by the Dutch Ministry of EL&I through the CATO2 program is acknowledged. The authors gratefully acknowledge Prof. Dr. Ir. M. van Sint Annaland (TU/e) for fruitful discussions. Dr. H. Li is kindly acknowledged for his contribution to the experiments.

References

[1] Ockwig NW, Nenoff TM. Chem Rev 2007;**107**(10): 4078.
[2] Lu GQ. J Colloid Interface Sci 2007;**314**(2):589.
[3] De Falco M. Chem Eng J 2007;**128**(2-3)115.
[4] De Falco M. Int. J Hydrogen Energy 2008; **33**(12):3036.
[5] Jansen D. Energy Procedia;2009 **1**(1);253.
[6] Boon J, Pieterse JAZ, Dijkstra JW, van Sint Annaland M. International Journal of Greenhouse Gas Control, 2012, accepted.
[7] Hysep. Hydrogen separation modules. http://www.hysep.com/, February 2012.
[8] Rusting, FT, De Jong G, Pex PPAC, Peters JAJP.WO0163162, August 2001.
[9] Jansen D, Dijkstra JW, Van den Brink RW, Peters TA, Stange M, Bredesen R, Goldbach A, Xu HY, Gottschalk A, Doukelis A. Energy Procedia 2009;**1**(1):253.
[10] Li H, Pieterse JAZ, Dijkstra JW, Haije WG, Xu HY, Bao C, Van den Brink RW, Jansen D. J Mem Sci 2011:**373**(1-2);43.
[11] Ward TL, Dao T. J Mem Sci 1999;**153**(2):211.
[12] Sieverts A, Krumbhaar W. Berichte der deutschen chemischen Gesellschaft 1910;**43**(1):893.
[13] Bhargav A, Jackson GS, Ciora RJ, Liu PTK. J Mem Sci 2010;**356**(1-2):123.
[14] Flanagan TB, Wang D. J Phys Chem C 2010;**114**(34):14482.
[15] Hara S, Ishitsuka M, Suda H, Mukaida M, Haraya K. J Phys Chem B 2009;**113**(29):9795.
[16] Skorpa R, Voldsund M, Takla M, Schnell SK, Bedeaux D, Kjelstrup S. J of Mem Sci 2012;**394-395**: 131.
[17] Krishna R, Wesselingh, JA. Chem Eng Sci 1997;**52**(6):861
[18] Mason EA, Lonsdale HK. J Mem Sci 1990;**51**(1-2):1.
[19]Rothenberger KS, Cugini AV, Howard BH, Killmeyer RP, Ciocco MV, Morreale BD, Enick RM, Bustamante F, Mardilovich IP, Ma YH. J Mem Sci 2004;**244**(1-2):55.
[20] Yun S, Oyama T. J Mem Sci 2011;**375**(1-2):28.

ECN
Westerduinweg 3
1755 LE Petten
The Netherlands

P.O. Box 1
1755 LG Petten
The Netherlands

T +31 88 515 4949
F +31 88 515 8338
info@ ecn.nl
www.ecn.nl